

# Frequency-selective near-field enhancement of radiative heat transfer via photonic-crystal slabs: a general computational approach

Alejandro W. Rodriguez,<sup>1,2</sup> Ognjen Ilic,<sup>3</sup> Peter Bermel,<sup>3</sup> Ivan Celanovic,<sup>3</sup>  
John D. Joannopoulos,<sup>3</sup> Marin Soljačić,<sup>3</sup> and Steven G. Johnson<sup>2</sup>

<sup>1</sup>*School of Engineering and Applied Sciences, Harvard University, Cambridge, MA 02138*

<sup>2</sup>*Department of Mathematics, Massachusetts Institute of Technology, Cambridge, MA 02139*

<sup>3</sup>*Department of Physics, Massachusetts Institute of Technology, Cambridge, MA 02139*

We describe an approach for computing the radiative heat transfer between arbitrarily-shaped bodies that is based on the stochastic finite-difference time-domain method. We employ this method to demonstrate the possibility of achieving enhanced frequency-selective near-field heat transfer between periodic photonic-crystal slabs at designable frequencies and separations. We find that the heat transfer can be further enhanced when the slabs are brought into a glide-symmetric configuration, a consequence of the degeneracies associated with the non-symmorphic symmetry group.

PACS numbers:

*Introduction:* We describe a finite-difference time-domain (FDTD) method to compute radiative heat transfer in the *near field* for arbitrary geometries and materials, and using this method we show that frequency-selective enhancement between thin slabs can be designed by the use of periodic photonic-crystal (PhC) structures, greatly exceeding the heat transfer attained using similar materials and geometries in the far field. Radiative (grey body) transfer of energy from a hot to a cold body, as shown schematically in Fig. 1, is well known to be enhanced (even exceeding the black-body limit) when the bodies are brought close enough for evanescent fields to contribute flux [1–7], but this *near-field transport* has thus far proven difficult to compute. Aside from semi-analytical results for planar structures [8–10], formulations have been developed that in principle handle arbitrary geometries but which thus far have only been evaluated using Fourier methods specialized only for pairs of spheres and/or plates [11–16]. However, in the far field it is well known that more complicated structures such as PhCs can be designed to resonantly enhance radiative transfer at desired frequencies [17–19], which is crucial for applications such as thermophotovoltaic cells in which only certain frequencies can be efficiently converted to power [19, 20]. Selectivity in the near field can be achieved by choosing materials that only absorb (and emit) at the desired wavelengths [9, 21, 22]. However, using *geometry* to achieve selectivity offers much greater control, since one can tailor the spectrum without finding new materials. In order to investigate arbitrary patterned geometries, we employ a rigorous yet intuitive approach: we directly simulate Maxwell’s equations with random thermal sources, an extension of the Langevin approach we previously used to model the emissivity of a single body [23] with additional modifications to handle nonequilibrium systems. In a simple model system consisting of two PhC slabs, thin films with periodic grooves [Fig. 2(top)], we show that the resonant modes created by the periodicity yield orders of magnitude enhancement in

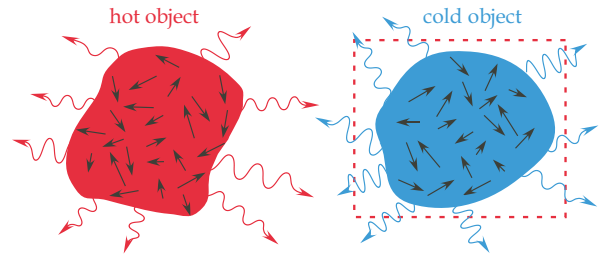


FIG. 1: Schematic of stochastic time-domain approach for computing the heat transfer between two arbitrarily shaped bodies, in which Maxwell’s equations are evolved in time in response to random thermal current sources (straight arrows) in the bodies, whose resulting electromagnetic fields (wiggly arrows) yield the steady-state flux spectrum around one of the bodies (dashed line).

the flux at designable wavelengths even for moderate separations (100s of nm to microns for infrared wavelengths) compared to similar structures in the far field, starting with weakly absorbing thin slabs that transfer  $< 1/1000$  of the flux between black bodies in the far field. Furthermore, we show that the selective enhancement can be almost doubled by using a glide-symmetric configuration [Fig. 3(bottom)], due to degeneracies resulting from the properties of the non-symmorphic symmetry group [24]. Ultimately, there is a tradeoff between enhancement and frequency selectivity—much larger enhancement is theoretically attained for nm separations [3–7] where geometric resonances have no effect, at the cost of frequency selectivity and much more difficult fabrication—and this letter offers a first glimpse of the practical design space that is available to optimize these considerations.

*Computational Method:* Given two arbitrarily shaped bodies (depicted schematically in Fig. 1), held at some arbitrary temperatures  $T_1 > T_2$ , our goal is to compute the radiative heat transfer  $h(\omega, T_1, T_2)$ , the net electromagnetic flux spectrum into a single body (e.g. through the dashed line in Fig. 1) from Planck-distributed ther-

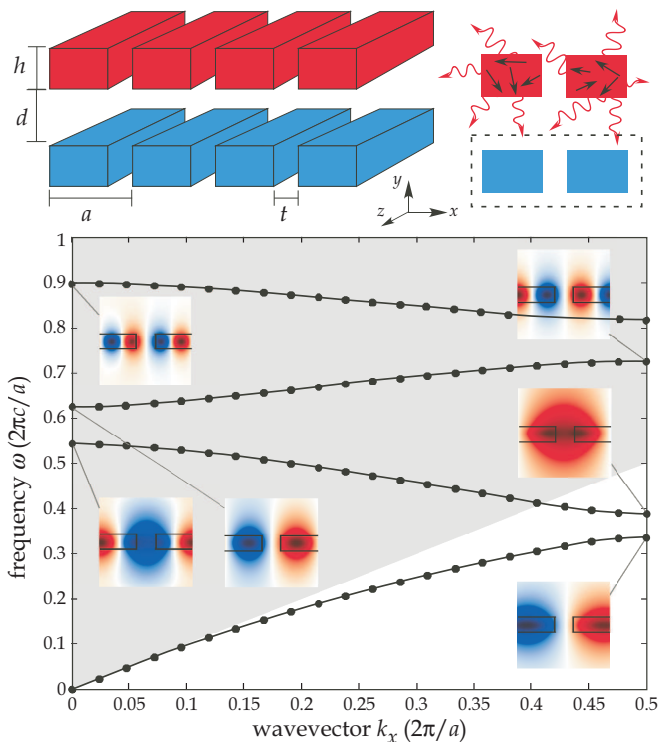


FIG. 2: (Top:) Schematic of a geometry consisting of two PhC dielectric slabs of thickness  $h = 0.2a$ , separated by a distance  $d$  in the  $y$  direction, each consisting of periodically repeated air grooves of period  $a$  and width  $t = 0.2a$  in the  $x$  direction. (Bottom:) Band diagram or frequency  $\omega$  of the TM ( $\mathbf{H} \cdot \hat{\mathbf{z}} = 0$ ),  $k_z = 0$  modes of an isolated slab as a function of  $k_x$ ; note the presence of both leaky (gray region) and guided modes. Insets depict the mode profiles at  $k_x = 0$  and  $k_x = \pi/a$ .

mal currents in both bodies [7]. More precisely, these Planck-distributed thermal currents can be explicitly expressed by a Langevin model [23], discussed below, and introduced as random sources in an FDTD simulation. We also exploit several further simplifications: the statistical independence of random currents in different bodies allows one to calculate thermal sources for one temperature at a time, linearity of electromagnetism permits the separation of the thermal distribution from the scattering calculation, and reciprocity allows us to omit sources in one of the two bodies entirely. In fact, the statistical independence of currents in different bodies is utilized in the standard definition of  $h$  [5]: the net transfer  $h = F_1(\omega, T_1) - F_2(\omega, T_2)$  is the flux  $F_1$  from sources only in body 1 radiating into body 2 minus the flux  $F_2$  from sources only in body 2 radiating into body 1.

The nature of the thermal sources is directly related to the nature of the material absorption via the fluctuation-dissipation theorem [25]. In FDTD, a Lorentzian or Drude peak in the absorption is modelled by coupling Maxwell's equations with a damped harmonic-oscillator equation for the corresponding polarization field [23]. In a Langevin approach, thermal sources are represented by

noise terms introduced as sources in these oscillator equations, which are uncorrelated in space but are temporally correlated so that the spectrum of each noise source is a Planck distribution  $\Theta(\omega, T) = \hbar\omega / [\exp(\hbar\omega/k_b T) - 1]$  at the local temperature  $T$  [5]. In principle, such correlated random sources—equivalent to uncorrelated (white) noise multiplied in the frequency domain by  $\sqrt{\Theta(\omega, T)}$ —can be generated directly, but this is computationally inconvenient. A key simplification results from the linearity of Maxwell's equations: if all the sources have the same temperature  $T$ , then instead of multiplying the *input* noise by  $\sqrt{\Theta}$  it is equivalent to employ white-noise sources and multiply the *output* fields by  $\sqrt{\Theta}$  (i.e., multiplying flux spectra by  $\Theta$ ). In previous work to simulate the thermal emission of a single body, we employed precisely this trick to use FDTD with white-noise sources in the polarization equations [23], and further details of the source implementation are described therein.

Therefore,  $F_j(\omega, T_j) = \Phi_j(\omega)\Theta(\omega, T_j)$ , where  $\Phi_j$  is the flux from white-noise sources in body  $j$  radiating into the other body. That is, statistical independence and linearity mean that we can perform two *temperature-independent* white-noise FDTD calculations, one for each body, to compute  $h = \Phi_1\Theta_1 - \Phi_2\Theta_2$ . This equation further simplifies due to reciprocity, which implies that  $\Phi_1 = \Phi_2$ . (Reciprocity equates the field generated at any point  $\mathbf{x}'$  in body 2 from a source at  $\mathbf{x}$  in body 1 with the fields at  $\mathbf{x}$  generated by a source at  $\mathbf{x}'$ ; as a consequence, the absorption at each point in body 2 from sources at each point in body 1 is equal to the corresponding absorption in 1 from 2, and when this is summed over all points one finds  $\Phi_1 = \Phi_2$ . In electrical networks, the corresponding principle is the symmetry of the mutual-impedance matrix.) Hence, one arrives at [4–7]:

$$h(\omega; T_1, T_2) = \Phi(\omega) [\Theta(\omega, T_1) - \Theta(\omega, T_2)], \quad (1)$$

where  $\Phi$  can be computed either from  $\Phi_1$  or  $\Phi_2$ . The  $\Phi_1 = \Phi_2$  relation also conveniently implies that Eq. (1) satisfies the second law of thermodynamics ( $h > 0$  at every  $\omega$  if and only if  $T_1 > T_2$ ), and in fact the second law conversely implies  $\Phi_1 = \Phi_2$ .

*Transfer between PhC slabs:* Using the Langevin approach outlined above, we investigate  $\Phi$  for the PhC structure shown in Fig. 2(top), involving two PhC dielectric slabs (thin films) of thickness  $h = 0.2a$ , separated by a distance  $d$  in the  $x$  direction, each consisting of  $z$ -oriented air grooves of period  $a$  and width  $t = 0.2a$  in the  $x$  direction. (This system is a proof of concept, not an optimized structure.) The permittivity of the slabs is taken to be of the Drude form  $\varepsilon(\omega) = \varepsilon_\infty - \sigma/\omega(\omega + i\gamma)$ , where  $\varepsilon_\infty = 12.5$ ,  $\sigma = 0.2533(2\pi c/a)^2$ , and  $\gamma = 1.5915(2\pi c/a)$ , approximating a dispersionless dielectric with  $\text{Re } \varepsilon \approx 12.5$  and  $\text{Im } \varepsilon \approx 1$  at wavelengths comparable to  $a$ .

The computation of  $\Phi$  for this structure, as outlined above, involves introducing uncorrelated white-

noise sources into the damped polarization equation [23] (responsible for the  $\varepsilon$  above, equivalent to a damped harmonic oscillator model with a frequency  $\rightarrow 0$ ) at each position (pixel) of one of the bodies [depicted as the red slab in Fig. 2(top)], and integrating the resulting flux spectrum over a surface surrounding the other slab [the blue slab in Fig. 2(top)]. We perform an ensemble average over many ( $N$ ) simulations, converging to the average  $\Phi$  as  $1/\sqrt{N}$  like any Monte-Carlo method, and we find that  $N = 80$  is sufficient to reduce the noise level in the spectrum to a few percent. By using a periodic unit cell in  $x$  with Bloch-periodic boundaries (phase difference  $e^{ik_x a}$ ) and integrating  $\Phi$  over  $k_x$ , we obtain the result for an infinite periodic structure. The  $y$  direction is truncated with standard PML absorbing layers [26]. The translation-invariant  $z$  direction can similarly be handled by integrating 2d simulations over  $k_z$ , but to simplify our initial model system we consider the 2d problem corresponding to  $k_z = 0$ . For  $k_z = 0$ , the electromagnetic fields can be decomposed into two non-interacting polarizations: TE ( $\mathbf{E} \cdot \hat{\mathbf{z}} = 0$ ) and TM ( $\mathbf{H} \cdot \hat{\mathbf{z}} = 0$ ). At the moderately large separations  $\lesssim a$  studied here (assuming  $a$  in the microns), we find that the TM contributions to the near-field heat transfer are more than an order of magnitude larger than the TE contributions (the opposite is known to occur at sufficiently small, e.g. nanometric, separations [6]), and so we focus exclusively on the TM modes and their contributions in the following discussion.

Before discussing the flux spectrum  $\Phi(\omega)$ , it is instructive to understand the modes of the isolated slabs. Figure 2 plots the (TM,  $k_z = 0$ ) band diagram or frequency  $\omega$  of the modes of a single isolated slab as a function of  $k_x$ . Modes that lie in the gray region (above the  $\omega = ck_x$  light line) are leaky modes [27], which radiate into the air and therefore contribute to heat transfer between the slabs in the far field. Modes that lie below the light line are guided modes [27], which evanescently decay in air and thus transfer energy only in the near field.

Figure 3(top) plots the flux enhancement  $\eta = \Phi_{t,d}/\Phi_{0,\infty}$  as a function of  $\omega$ , where  $\Phi_{t,d}(\omega)$  is the flux spectrum between PhC slabs of groove width  $t$  and separated by distance  $d$ , here normalized by the flux spectrum  $\Phi_{0,\infty}$  of the unpatterned slabs ( $t = 0$ ) in the far field ( $d \rightarrow \infty$ ) to clearly illustrate the effect of finite  $t$  and  $d$ . The calculation of  $\Phi_{0,\infty}$  is simplified due to the well-known expression  $\Phi_{0,\infty} = A^2/(1 - R^2)$ , relating the heat transfer in the far field to the absorptivity  $A$  and reflectivity  $R$  of each unpatterned slab [3], which can be computed by standard transfer-matrix methods. (Calculations using our stochastic method for  $d = 8a$  yields results almost identical to the  $d \rightarrow \infty$  limit.) The  $\Phi_{0,\infty}(\omega)$  spectrum by itself is nearly flat, so the spectral features in Fig. 3 are not due to the normalization. We should also point out that we are starting with very weakly absorbing slabs (thin films), i.e.  $\Phi_{0,\infty}$  is more than 1000

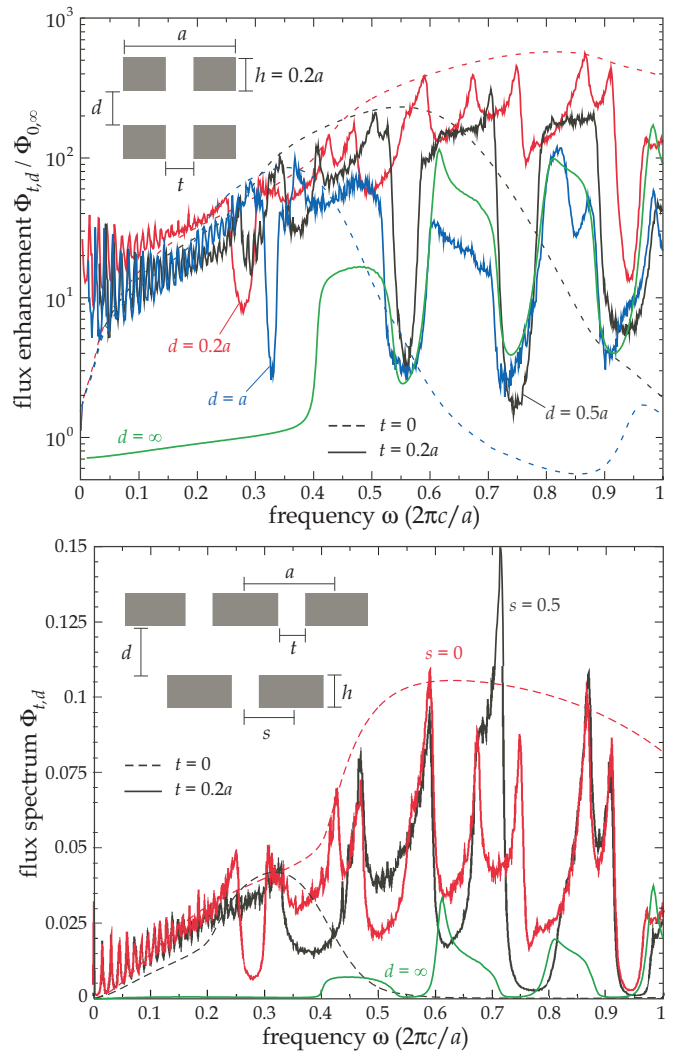


FIG. 3: (Top:) Plot of flux enhancement  $\eta = \Phi_{t,d}/\Phi_{0,\infty}$  as a function of  $\omega$  (units of  $2\pi c/a$ ), where  $\Phi_{t,d}$  is the flux spectrum between PhC slabs of groove width  $t$  and separation  $d$  (depicted in Fig. 2), plotted for various  $d$ . Solid (dashed) lines correspond to  $\eta$  for patterned (unpatterned) slabs, i.e. width  $t = 0.2a$  ( $t = 0$ ). Red, black, blue, and green denote different separations  $d = 0.2a, 0.5a, a$ , and the limit  $d \rightarrow \infty$ , respectively. (Bottom:) Flux spectrum  $\Phi_{t,0.2a}$  in a symmetric ( $s = 0$ , red line) or glide-symmetric ( $s = 0.5a$ , black line) slab-slab configuration. Green line corresponds to the far-field spectrum  $\Phi_{0.2a,\infty}$ .

times smaller than the  $\Phi = 1$  of two black bodies.

The fact that radiative heat transfer can be significantly changed by the periodicity of the slabs [18] is illustrated by the green curve in Fig. 3(top), which shows  $\eta$  for PhCs of groove width  $t = 0.2a$  in the far field. As shown,  $\Phi_{0.2a,\infty}$  exhibits a number of wide-bandwidth peaks as a function of  $\omega$ , whose magnitude are orders of magnitude larger than  $\Phi_{0,\infty}$ . Not surprisingly, the bandwidth of these peaks exactly matches the bandwidth of the leaky-mode bands in Fig. 2(bottom), whose inte-

grated contribution over all  $k_y$  leads to a smearing of the sharp spectral peaks that occur at the leaky-mode frequencies for each  $k_y$ . The sharp drop in  $\eta$  between the peaks is a consequence of the presence of band gaps (technically pseudogaps) between the leaky-mode bands.

As the separation between the slabs decreases, a number of dramatic features are observed in Fig. 3(top), which shows  $\eta$  at three additional separations ( $d = 0.2a$ ,  $d = 0.5a$  and  $d = a$ ). At  $d = a$ , one can observe a dramatic increase in  $\eta$  at low frequencies. This arises due to the increased coupling and contribution of guided modes to  $h$ . This near-field coupling increases further at smaller  $d$ , and additionally (especially in the  $d = 0.2a$  curve) one can see a dip corresponding to the gap in the guided modes of Fig. 2(bottom), and peaks at the edges of the gap (where the vanishing group velocity gives rise to a van Hove singularity in the local density of states [27]). There is also an enhancement of  $\Phi$  at small  $d$  for the leaky-mode peaks, because leaky modes in a patterned slab have an evanescent as well as a radiative component [27], and the former enhances the coupling at short distances. (Note, however, that the enhancement is not generally monotonic in  $d$ .) Second, the leaky modes split into bonding and antibonding pairs as  $d$  decreases (and a similar splitting will be visible in the guided modes at even smaller  $d$ ), causing the peaks to split into two (a phenomenon visible even more clearly in the linear-scale plot of Fig. 3(bottom), discussed below).

Figure 3(top) also shows the enhancement for unpatterned ( $t = 0$ ) slabs. These also exhibit a striking near-field enhancement for  $d < a$ , but in this case the enhancement is broad-band, because there are no standing-wave leaky-mode solutions in an unpatterned slab to induce frequency selectivity. At large separations (e.g.  $d = a$ ), the patterned slab exhibits more than 10 times the enhancement of the unpatterned slab, due to these resonant contributions. At  $d = 0.5a$ , the unpatterned slab is better for small  $\omega$  and is worse for larger  $\omega$ , where the latter is due to the fact that the evanescent interactions become shorter and shorter range at high  $\omega$  and vanish in the absence of resonant enhancement. At  $d = 0.2a$ , the unpatterned slab has larger enhancement over the whole bandwidth shown here, but lacks frequency selectivity. (At even smaller  $d$ , not shown, the periodic structure ceases to matter and the interactions can be described by a proximity approximation in which adjacent surfaces are treated as parallel plates [4–7]; in this limit the patterned  $\Phi$  will be smaller by a factor of  $1 - t/a$ .)

A striking enhancement in the near-field interaction occurs when one patterned slab is shifted in the  $x$  direction by  $0.5a$  with respect to the other slab, as shown in Fig. 3(bottom). In this case (plotted here as absolute  $\Phi$  on a linear scale), the bonding-antibonding split peaks of the original patterned  $\Phi$  (solid red curves) *merge* in some cases and *add* to approximately double the heat transfer, even exceeding that of the unpatterned slab. The reason

for this is that the shifted structure is glide-symmetric, and the resulting non-symmorphic symmetry group is known to support degeneracies at the Brillouin zone edge ( $k = \pi/a$ ) [24], so the bonding-antibonding splittings corresponding to the  $k = \pi/a$  modes disappear. (On the other hand, the frequency splitting corresponding to the  $k = 0$  band edges, e.g. at  $\omega = 0.9 (2\pi c/a)$ , persists even for the glide-symmetric structure.) Similarly, the gap in the guided modes of Fig. 2(bottom), from  $\omega \approx 0.33$ – $0.39 (2\pi c/a)$  is greatly modified by the presence of the other slab in the mirror-symmetric case (red curve) but not in the glide-symmetric case (grey curve), again due to the lack of interaction at  $k = \pi/a$ . (In contrast, we have also computed the heat transfer from a patterned slab to an unpatterned slab—while there is no splitting of the peaks, there is no adding of the peaks either and the  $\Phi$  is worse than the mirror-symmetric case.)

The overall frequency-selective enhancement brings the heat transfer from 1/1000 of a black body (in the far field, for unpatterned slabs) to 15% of a black body (in the near field, for patterned slabs), at very moderate separations (if the peak enhancement is a wavelength of  $10 \mu\text{m}$ , then  $a = 7 \mu\text{m}$  and  $d = 1.4 \mu\text{m}$ ). Even larger absolute frequency-selective performance could be expected if we further optimized the parameters, e.g. if we started with a far-field structure whose efficiency was not so poor.

- 
- [1] J. J. Loomis and H. J. Maris, Phys. Rev. B **50**, 18517 (1994).
  - [2] J. B. Pendry, J. Phys.: Condens. Matter **11**, 6621 (1999).
  - [3] M. Phillipe-Jean, K. Joulain, R. Carminati, and J.-J. Greffet, Micro. Therm. Eng. **6**, 209 (2002).
  - [4] K. Joulain, J.-P. Mulet, F. Marquier, R. Carminati, and J.-J. Greffet, Surf. Sci. Reports **57**, 59 (2005).
  - [5] A. I. Volokitin and B. N. J. Persson, Rev. Mod. Phys. **79**, 1291 (2007).
  - [6] Z. M. Zhang, *Nano/Microscale heat transfer* (McGraw-Hill, 2007).
  - [7] S. Basu, Z. M. Zhang, and C. J. Fu, Int. J. Energy Res. **33**, 1203 (2009).
  - [8] S. A. Biehs, Eur. Phys. J. B **58**, 423 (2007).
  - [9] C. Fu and W. Tan, Journal of Quantitative Spectroscopy and Radiative Transfer **110**, 1027 (2009).
  - [10] W. T. Lau, J.-T. Shen, G. Veronis, and S. Fan, Phys. Rev. B **80**, 155135 (2009).
  - [11] A. Narayanaswamy and G. Chen, Phys. Rev. B **77**, 075125 (2008).
  - [12] G. Bimonte, Phys. Rev. A **80**, 042102 (2009).
  - [13] S.-B. Wen, J. Heat Transfer **132**, 072704 (2010).
  - [14] R. Messina and M. Antezza, arXiv **1012.5183**, 1 (2011).
  - [15] M. Kruger, T. Emig, and M. Kardar, arXiv **1102.3890**, 1 (2011).
  - [16] C. Otey and S. Fan, arXiv **1103.2668**, 1 (2011).
  - [17] J.-J. Greffet, R. Carminati, K. Joulain, J.-P. Mulet, S. Mainguy, and Y. Chen, Nature **416**, 61 (2001).
  - [18] D. L. C. Chan, M. Soljačić, and J. D. Joannopoulos, Phys. Rev. E **74**, 016609 (2006).

- [19] P. Bermel, et al., *Optics Express* **18**, A314 (2010).
- [20] M. Whale and E. Cravalho, *Energy Conversion, IEEE Transactions on* **17**, 130 (2002).
- [21] M. Francoeur, M. P. Menguc, and R. Vaillon, *Appl. Phys. Lett.* **93**, 043109 (2008).
- [22] S. Shen, A. Narayanaswamy, and G. Chen, *Nano Letters* **9**, 2909 (2009).
- [23] C. Luo, A. Narayanaswamy, G. Ghen, and J. D. Joannopoulos, *Phys. Rev. Lett.* **93**, 213905 (2004).
- [24] A. Mock, L. Lu, and J. O'Brien, *Phys. Rev. B* **81**, 155115 (2010).
- [25] S. M. Rytov, V. I. Tatarskii, and Y. A. Kravtsov, *Principles of Statistical Radiophysics II: Correlation Theory of Random Processes* (Springer-Verlag, 1989).
- [26] A. Taflove and S. C. Hagness, *Computational Electrodynamics: The Finite-Difference Time-Domain Method* (Artech, Norwood, MA, 2000).
- [27] J. D. Joannopoulos, S. G. Johnson, J. N. Winn, and R. D. Meade, *Photonic Crystals: Molding the Flow of Light* (Princeton University Press, 2008), 2nd ed.